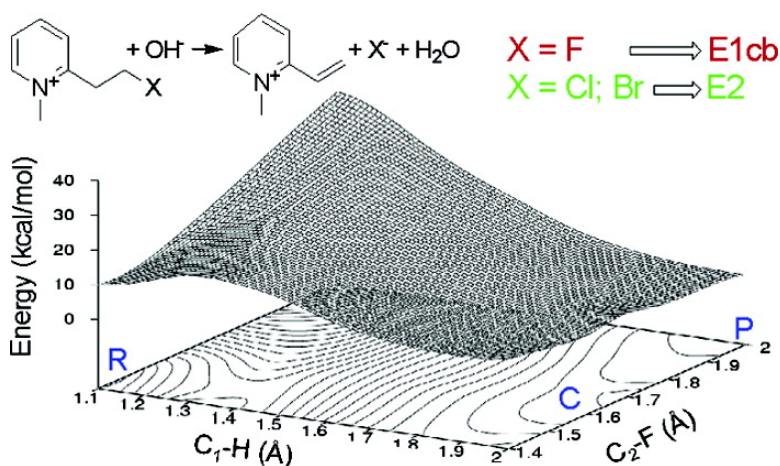


Evidence of a Borderline Region between E1cb and E2 Elimination Reaction Mechanisms: A Combined Experimental and Theoretical Study of Systems Activated by the Pyridine Ring

Sergio Alunni, Filippo De Angelis, Laura Ottavi, Magdalini Papavasileiou, and Francesco Tarantelli

J. Am. Chem. Soc., 2005, 127 (43), 15151-15160 • DOI: 10.1021/ja0539138 • Publication Date (Web): 11 October 2005

Downloaded from <http://pubs.acs.org> on March 25, 2009



More About This Article

Additional resources and features associated with this article are available within the HTML version:

- Supporting Information
- Links to the 3 articles that cite this article, as of the time of this article download
- Access to high resolution figures
- Links to articles and content related to this article
- Copyright permission to reproduce figures and/or text from this article

[View the Full Text HTML](#)

Evidence of a Borderline Region between E1cb and E2 Elimination Reaction Mechanisms: A Combined Experimental and Theoretical Study of Systems Activated by the Pyridine Ring

Sergio Alunni,^{*,†} Filippo De Angelis,^{*,‡} Laura Ottavi,[†] Magdalini Papavasileiou,[†] and Francesco Tarantelli^{†,‡}

Contribution from the Dipartimento di Chimica, Università di Perugia, Via Elce di Sotto 8, I-06213, Perugia, Italy, and Istituto CNR di Scienze e Tecnologie Molecolari (ISTM), c/o Dipartimento di Chimica, Università di Perugia, Via elce di Sotto 8, I-06213, Perugia, Italy

Received June 14, 2005; E-mail: alunni@unipg.it; filippo@thch.unipg.it

Abstract: We report a combined experimental and theoretical study to characterize the mechanism of base-induced β -elimination reactions in systems activated by the pyridyl ring, with halogen leaving groups. The systems investigated represent borderline cases, where it is uncertain whether the reaction proceeds via a carbanion intermediate (E1cb, $A_{\text{XH}}D_{\text{H}} + D_{\text{N}}$) or via the concerted loss of a proton and the halide (E2, $A_{\text{N}}D_{\text{E}}D_{\text{N}}$) upon base attack. Experimentally, the Taft correlation for H/D exchange, in $\text{OD}^-/\text{D}_2\text{O}$ with noneliminating substrates (1-methyl-2-(2-Xethyl)pyridinium iodide), is used to predict the expected values of the rate constants for the elimination reactions with *N*-methylated substrates and F, Cl, Br as the leaving group. The comparison indicates an E1cb irreversible mechanism with F, but the deviation observed with Cl and Br does not allow a conclusive assignment. The theoretical calculations show that for the *N*-methylated substrate with a fluoride leaving group the elimination proceeds via formation of a moderately stable carbanion. No stable anionic intermediate is instead found when the leaving group is Cl or Br, as well as for any of the nonmethylated species, indicating a concerted elimination. The methylated substrate with Cl shows however only a moderate increase in reactivity compared to the fluorinated substrate, despite the change in mechanism. Very interestingly, our analysis of the computed two-dimensional potential energy surface for the reaction with a F leaving group indeed evidences the lack of a net distinction between the E1cb and E2 reaction paths, which appear to merge smoothly into each other in these borderline cases.

Introduction

Base-induced β -elimination reactions, with formation of a carbon–carbon double bond, are one of the most fundamental chemical reactions and of recognized importance in the understanding of the mechanisms with which they take place in different substrates and solution environments. In particular, being able to distinguish between concerted and stepwise mechanisms is a very relevant issue in both chemistry^{1–13} and biochemistry.¹⁴ However, the nature of the borderline between concerted and stepwise mechanisms is yet unclear,^{5,15} and an

obviously important aspect of this problem is establishing whether there is smooth continuity or distinct discontinuity between the E2 concerted and the E1cb stepwise mechanisms. The distinction between the E2 concerted process ($A_{\text{XH}}D_{\text{H}}D_{\text{N}}$) and the E1cb irreversible mechanism ($A_{\text{XH}}D_{\text{H}}^* + D_{\text{N}}$) is a difficult task.^{1,5,15} In fact, while the E1cb reversible mechanism

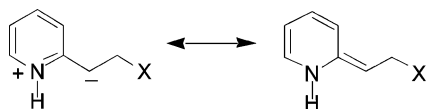
[†] Dipartimento di Chimica.

[‡] Istituto CNR di Scienze e Tecnologie Molecolari (ISTM).

- (1) (a) Saunders, W. H., Jr.; Cockerill, A. F. *Mechanism of Elimination Reaction*; Wiley-Interscience Publication: New York, 1973; Vol. II, pp 60–68. (b) Baciocchi, E. *The Chemistry of Halides, Pseudo Halides and Azides, Supplement D*; Patai, S., Rappoport, Z., Eds.; Wiley: Chichester, UK; 1983. (c) Gandler, J. R. *The Chemistry of Double Bonded Functional Group*; Patai, S., Eds.; Wiley: Chichester, UK, 1989. (d) Saunders, W. H., Jr. *Acc. Chem. Res.* **1976**, *9*, 19. (e) Stirling, C. J. M. *Acc. Chem. Res.* **1979**, *12*, 198. (f) Cavestri, R. C.; Fedor, L. R. *J. Am. Chem. Soc.* **1970**, *92*, 4610. (g) Fedor, L. R.; Glave, W. R. *J. Am. Chem. Soc.* **1971**, *93*, 985.
- (2) (a) Gandler, J. R.; Storer, W. J.; Ohlberg, D. A. *J. Am. Chem. Soc.* **1990**, *112*, 7756. (b) Gandler, J. R.; Yokoyama, T. *J. Am. Chem. Soc.* **1984**, *106*, 130.
- (3) Gandler, J. R.; Jencks, W. P. *J. Am. Chem. Soc.* **1982**, *104*, 1937.
- (4) (a) Thibblin, A. *J. Am. Chem. Soc.* **1989**, *111*, 5412. (b) Meng, Q.; Thibblin, A. *J. Am. Chem. Soc.* **1995**, *117*, 1839. (c) Meng, Q.; Thibblin, A. *J. Am. Chem. Soc.* **1995**, *117*, 9399.

- (5) (a) More O'Ferrall, R. A.; Warren, P. J. *J. Chem. Soc., Chem. Commun.* **1975**, 483. (b) More O'Ferrall, R. A.; Warren, P. J.; Ward, P. M. *Acta University Uppsol., Symp. University Uppsol.* **1978**, *12*, 209.
- (6) More O'Ferrall, R. A.; Larkin, F.; Walsh, P. *J. Chem. Soc., Perkin Trans. 2* **1982**, 1573.
- (7) Larkin, F.; More O'Ferrall, R. A. *Aust. J. Chem.* **1983**, *36*, 1831.
- (8) Thibblin, A. *J. Am. Chem. Soc.* **1988**, *110*, 4582.
- (9) Ölwegård, M.; McEwen, I.; Thibblin, A.; Ahlberg, P. *J. Am. Chem. Soc.* **1985**, *107*, 7494.
- (10) Jencks, W. P. *Chem. Soc. Rev.* **1981**, *10*, 345.
- (11) Marshall, D. R.; Thomas, P. J.; Stirling, C. J. M. *J. Chem. Soc., Perkin Trans. 2* **1977**, 1914.
- (12) Banait, N. S.; Jencks, W. P. *J. Am. Chem. Soc.* **1990**, *112*, 6950.
- (13) (a) Thibblin, A. *Chem. Soc. Rev.* **1993**, 427. (b) Jencks, W. P. *Acc. Chem. Res.* **1980**, *13*, 1. (c) Cho, B. R.; Kim, Y. K.; Yoon, C.-O. *M. J. Am. Chem. Soc.* **1997**, *119*, 691. (d) Koch, H. F., et al. *J. Am. Chem. Soc.* **1997**, *119*, 9965 (Supporting Information available for complete ref 13d); (e) Koch, H. F.; McLennan, D. J.; Koch, J. G.; Tumas, W.; Dobson, B.; Koch, N. H. *J. Am. Chem. Soc.* **1983**, *105*, 1930. (f) Koch, H. F.; Koch, J. G.; Koch, N. H.; Koch, A. S. *J. Am. Chem. Soc.* **1983**, *105*, 2388.
- (14) (a) Abeles, R. H.; Frey, P. A.; Jencks, W. P. *Biochemistry*; Jones and Bartlett Publisher: 1992. (b) Voet, D.; Voet, J. G. *Biochemistry*; John Wiley & Sons: 1990.
- (15) Larkin, F. G.; More O'Ferrall, R. A.; Murphy, D. G. *Collect. Czech. Chem. Commun.* **1999**, *64*, 1833.

Scheme 1



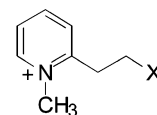
($A_{\text{XH}}D_{\text{H}} + D_{\text{N}}^*$) can be revealed¹ by the presence of H/D exchange,¹⁶ by studies of acid–base catalysis¹⁶ and by the inverse solvent isotope effect,^{16b,17} the E2 mechanism shows many of the same characteristics of an E1cb irreversible mechanism. In previous studies^{16a,17–20} of β -elimination reactions in systems activated by the pyridine ring, we have reported a high value of the Proton Activating Factor, PAF, defined as the ratio of the second-order rate constant for the nitrogen protonated substrate, NH^+ , and that for the unprotonated substrate, N (PAF = $k^{\text{NH}^+}/k^{\text{N}}$). The value found with 2-(2-fluoroethyl)pyridine¹⁹ is PAF = 3.6×10^5 (acetohydroxamate base, 50 °C, $\mu = 1$ M KCl), whereas with *N*-[2-(2-pyridyl)ethyl]quinuclidinium PAF is 5.2×10^5 . The high values of PAF observed were interpreted in terms of an E1cb mechanism and a strongly resonance-stabilized intermediate carbanion; see Scheme 1.

Activation by methylation^{19,20} of the N atom of the pyridine ring is also strong, similar to protonation. However, several uncertainties remain about the β -elimination in these borderline systems. The reaction mechanism itself has not yet been determined with certainty, nor has it been ascertained whether a change of mechanism takes place with different X leaving groups or upon going from the unprotonated to the protonated substrate. There are several biological processes where the effect of stabilization of a carbanion by a quaternized nitrogen atom, part of a heteroaromatic system, is important. One example¹⁴ is the mechanism of action of a cofactor related to the B6 vitamin, the pyridoxal phosphate. In this system, the protonated pyridine ring provides the necessary stabilization of the intermediate carbanion formed in the elimination, transamination, decarboxylation, and racemization reactions involving this cofactor in the amino acids metabolism. Another¹⁴ example is the chemistry of thiamine pyrophosphate, where the carbanion formed in the decarboxylation of α -ketoacids presents an enamine-type structure. Also the enzymatic β -elimination reaction of ammonia from L-histidine, catalyzed by Histidine Ammonia-Lyase, is proposed to occur by an E1cb mechanism with activation provided by the nitrogen-protonated imidazole ring.²¹

Previous theoretical studies on β -elimination reactions have mainly focused on prototype substrates (mostly $\text{CH}_3\text{CH}_2\text{X}$, with X = halogen) and were generally limited to the gas phase.^{22–26} Among the many different theoretical studies, of particular relevance is the series performed by Gronert,²² Saunders,²⁴ and Jensen²⁵ using mainly ab initio (MP2–MP4) calculations. Bickelhaupt et al.²³ performed a two-dimensional scan of the potential energy surface for the $\text{CH}_3\text{CH}_2\text{F}$ substrate using

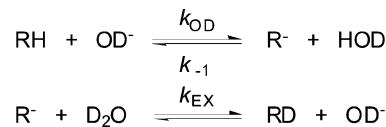
- (16) (a) Alunni, S.; Conti, A.; Palmizio Errico, R. *J. Chem. Soc., Perkin Trans. 2* **2000**, 453. (b) Keeffe, J. R.; Jencks, W. P. *J. Am. Chem. Soc.* **1983**, *105*, 265.
 (17) Alunni, S.; Conti, A.; Palmizio Errico, R. *Res. Chem. Intermed.* **2001**, *27*, 653.
 (18) Alunni, S.; Busti, A. *J. Chem. Soc., Perkin Trans. 2* **2001**, 778.
 (19) Alunni, S.; Laureti, V.; Ottavi, L.; Ruzziconi, R. *J. Org. Chem.* **2003**, *68*, 718.
 (20) Alunni, S.; Ottavi, L. *J. Org. Chem.* **2004**, *69*, 2272.
 (21) Langer, M.; Pauling, A.; Rétey J. *Angew. Chem., Int. Ed Engl.* **1995**, *34*, 1464.

Scheme 2



X = H (1), CH₃ (2), Ph (3), OH (4), OEt (5)

Scheme 3



Density Functional Theory (DFT) calculations. More recently, the $\text{CH}_3\text{CH}_2\text{F}$ substrate has been the subject of extensive theoretical investigations based on ab initio molecular dynamics simulations in the gas phase,²⁶ aimed at providing a detailed description of the free-energy landscape for the competing elimination/substitution reactions.

In this paper we report the results of a combined experimental and theoretical study, based on DFT calculations in solution, aimed at understanding some important aspects of the borderline region between E1cb and E2 reaction mechanisms in systems activated by the pyridine ring. We have studied 2-(2-fluoroethyl)pyridine and its chlorine and bromine analogues, with and without methyl activation at the nitrogen. Work is in progress to investigate the related elimination reactions for the isomers with the ethyl moiety in position 3 and 4.

Result and Discussion

Experimental Study. Second-order rate constants, k_{OD} , $\text{M}^{-1} \text{s}^{-1}$, for H/D exchange with substrates **1–5** (Scheme 2) have been measured by following the disappearance of the exchangeable protons (Py-CH_2), in $\text{OD}^-/\text{D}_2\text{O}$ at 25 °C, $\mu = 1$ M KCl, by NMR spectroscopy.

In these conditions the concentration of OD^- is constant owing to the reaction of the carbanion with D_2O (Scheme 3).

The k_{OD} values were calculated from the equation $\ln(I_0/I_t) = k_{\text{OD}}[\text{OD}^-] \times \text{time}$, where I_0 is the integration ratio between the signals of exchangeable hydrogens and that of a reference signal at time = 0; I_t is the same ratio at time = t . This treatment assumes that there are not α -secondary isotope effects on exchange, but these are expected to be very small.²⁷ The k_{OD} values are reported in Table 1.

- (22) (a) Gronert, S. *J. Am. Chem. Soc.* **1991**, *113*, 6041. (b) Gronert, S. *J. Am. Chem. Soc.* **1992**, *114*, 2349. (c) Gronert, S. *J. Am. Chem. Soc.* **1993**, *115*, 652. (d) Gronert, S.; Merrill, G. N.; Kass, S. R. *J. Org. Chem.* **1995**, *60*, 488. (e) Gronert, S.; Freed, P. *J. Org. Chem.* **1996**, *61*, 9430. (f) Gronert, S.; Kass, S. R. *J. Org. Chem.* **1997**, *62*, 7991. (g) Merrill, G. N.; Gronert, S.; Kass, S. R. *J. Phys. Chem. A* **1997**, *101*, 208.
 (23) Bickelhaupt, F. M.; Baerends, E. J.; Nibbering, N. M. M.; Ziegler, T. *J. Am. Chem. Soc.* **1993**, *115*, 9160.
 (24) (a) Saunders, W. H., Jr. *J. Org. Chem.* **1997**, *62*, 244. (b) Saunders, W. H., Jr. *J. Org. Chem.* **1999**, *64*, 861. (c) Saunders, W. H., Jr. *J. Org. Chem.* **2000**, *65*, 681.
 (25) (a) Glad, S. S.; Jensen F. *J. Am. Chem. Soc.* **1994**, *116*, 9302. (b) Glad, S. S.; Jensen F. *J. Phys. Chem.* **1996**, *100*, 16892. (c) Glad, S. S.; Jensen F. *J. Phys. Chem.* **1997**, *62*, 2253.
 (26) (a) Mugnai, M.; Cardini, M.; Schettino, V. *J. Phys. Chem. A* **2003**, *2540*. (b) Ensing, B.; Laio, A.; Gervasio, F. L.; Parrinello, M.; Klein, M. L. *J. Am. Chem. Soc.* **2004**, *126*, 9492. (c) Ensing, B.; Klein, M. L. *Proc. Natl. Acad. Sci.* **2005**, *102*, 6755.
 (27) Altson, W. C.; Haley, K.; Kanski, R.; Murray, C. J.; Pranata, J. *J. Am. Chem. Soc.* **1996**, *118*, 6562.

Table 1. Second-Order Rate Constants, k_{OD} , $M^{-1} s^{-1}$, for H/D Exchange with Substrates 1–5 (Scheme 2) in OD^-/D_2O , 25 °C, $\mu = 1$ M KCl and Second-Order Rate Constants, k_E , $M^{-1} s^{-1}$, for the β -Elimination Reactions with 1-Methyl-2-(2-xethyl)pyridinium iodide in OH^-/H_2O , 25 °C, $\mu = 1$ M KCl

X	$k_{OD}/M^{-1} s^{-1}$	$k_E/M^{-1} s^{-1}$	σ^{*b}
H (1)	0.0105		0
CH ₃ (2)	0.0087		-0.1
Ph (3)	0.039		0.215
OH (4)	0.37		0.555
OEt (5)	0.65		0.577 ^c
F		10.25	1.1
Cl		25.2 ^d	1.05
Br		78.5	1.0
OTs		81	1.31 ^e

^a Average value of three determinations at three different $[OD^-]$; the error is $\pm 7\%$. ^b Reference 28. ^c The value of σ^* for OEt is calculated from the value of $\sigma_1 = 0.26$ and the relation $\sigma_1 = 0.45 \times \sigma^*$ (ref 29). ^d Previously (ref 18), we have reported a value of $17.9 M^{-1} s^{-1}$, but the value of this work was more accurately determined by stopped-flow. ^e Calculated from a σ_1 value = 0.59.

In this system k_{OD} is the second-order rate constant for carbanion formation, Scheme 3. In fact, the use of steady-state approximation, with $k_{ex} > k_{-1}$, implies k_{OD} rate determining, and $k_{obs} = k_{OD}[OD^-]$. We have excluded that in our systems there is significant internal return^{13d-f} from the R⁻-HOD intermediate on the base of the following reasons:

(1) We have previously¹⁹ discussed, and this work confirms this point, that the mechanism of the elimination reaction induced by OH^- with 1-methyl-2-(2-fluoroethyl)pyridinium iodide is E1cb irreversible. The second-order rate constant for carbanion formation k_{OH} at 25 °C, $\mu = 1$ M KCl is $10.25 M^{-1} s^{-1}$. As the pK_a for the β hydrogens with respect to F is of the order of 18 (see below), then it can be calculated a value of k_{H_2O} , the first-order rate constant for protonation of the carbanion by H_2O , of $\sim 10^5 s^{-1}$. This value is several orders of magnitude lower than 10^{11} , the first-order rate constant for solvent reorganization; in the case of significant internal return, solvent reorganization would be rate determining in the direction of carbanion protonation.³⁰ Similar calculations with k_{OD} (Table 1) give estimated values for deuteration of the carbanion significantly lower than $10^{11} s^{-1}$.

(2) It has been reported³⁰ that, for deprotonation of CH_3CN , internal return competes with solvent reorganization; the pK_a value of this substrate is 28.9. If our systems have a pK_a several orders of magnitude lower, then the barrier for the reprotonation is much larger and the internal return should not compete with solvent reorganization, so the rate determining in the H/D exchange direction is expected to be carbanion formation (k_{OD}).

Stirling¹¹ and More O'Ferrall¹⁵ have shown that it is possible to use the Taft equation²⁸ to predict the expected values of the second-order rate constant for the E1cb irreversible mechanism of related substrates. If the line of the Taft correlation of rates of isotope exchange with noneliminating substrates is related to the carbanion formation rates, then it is possible to predict the rate (k_E) of an E1cb irreversible mechanism with eliminating substrates provided the σ^* of the leaving group is known. So if the observed value of k_E is in agreement with the predicted value of the Taft plot, the mechanism can be assigned as E1cb

(28) Taft, R. W. *Steric Effect in Organic Chemistry*; Newman, M., Ed.; Wiley: New York, 1956.

(29) Shorter, J. *Correlation Analysis in Chemistry*; Chapman, N. B., Shorter, J., Eds.; Plenum: London, 1978.

(30) Richard, J. P.; Williams, G.; Gao, J. *J. Am. Chem. Soc.* **1999**, *121*, 715.

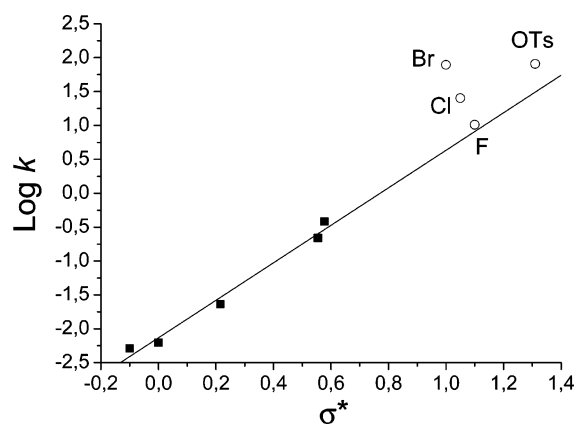


Figure 1. Taft plot $\log(k_{OD}/1.7)$ vs σ^* for H/D exchange with substrates 1–5, solid square; linear regression analysis gives $\log(k_{OD}/1.7) = -2.13$ (sd = 0.08) + 2.77 (sd = 0.2) σ^* . The open circles are $\log(k_E)$ for the elimination reactions for the methylated substrates with the indicated leaving group.

irreversible, while if the value k_E is significantly larger, an E2 concerted mechanism can be assigned. We have used this approach, and we have measured the rate of H/D exchange with substrates 1–5 in OD^-/D_2O , 25 °C, $\mu = 1$ M KCl. As previously discussed, the measured k_{OD} represents the second-order rate constant for carbanion formation. However, it is to be considered that we have measured k_{OD} in OD^-/D_2O , while the k_E constants are measured in OH^-/H_2O . The ratio k_{OD}/k_{OH} can vary³⁰⁻³² from 1 to 2.4. In our case, where the substrate deprotonation is rate determining, it can be assumed an average factor of 1.7; so k_{OD} (OD^-/D_2O) are divided by 1.7 to give $k_{OD}/1.7$ (OH^-/H_2O). It is also to be considered that our k_{OD} values, measured as described in the Experimental Section, refer to the rate constants for the exchange of 1H (the two H of the CH_2 systems are both exchanged). In Figure 1 is shown the Taft plot ($\log k_{OD}/1.7$ against σ^*) with substrates 1–5.

A good correlation is observed with substrates 1–5, $\log(k_{OD}/1.7) = -2.13$ (sd = 0.08) + 2.77 (sd = 0.2) σ^* . In Figure 1 are also shown the values of $\log k_E$ for the antielimination reactions with the methylated substrates at 25 °C, $\mu = 1$ M KCl and with leaving groups F, Cl, Br, OTs. The value of $\rho^* = +2.77$ is similar to the one reported with 9-methylfluorenes, $\rho^* = +2.6$.¹⁵ The ratio $k_{measured}/k_{predicted}$ for the elimination reactions are 1.2 (X = F), 4.2 (X = Cl), 18 (X = Br), 2.6 (X = OTs). The deviation from the Taft plot with the halogens leaving group is shown in Figure 2.

From the deviation observed in the Taft plot it can be concluded that with leaving group F the mechanism is E1cb irreversible; with Cl and Br the deviations observed are small and could be related to the switch to the E2 concerted mechanism or to negative hyperconjugation^{8,9,24,33} within an (E1cb)₁ mechanism. This effect involves some lengthening of the C–X bond in the intermediate carbanion. We have previously¹⁹ assigned an (E1cb)₁ mechanism with 1-methyl-2-(2-

(31) Kresge, A. J.; More O'Ferrall, R. A.; Powell, M. F. *Isotopes in Organic Chemistry*; Buncl, E., Lee, C. L., Eds.; Elsevier, New York, 1987.

(32) (a) Steffa, L. J.; Thornton, A. R. *J. Am. Chem. Soc.* **1967**, *89*, 6149. (b) Showen, R. L. *Prog. Phys. Org. Chem.* **1972**, *9*, 275.

(33) (a) Thibblin, A.; Ahlberg, P. *J. Am. Chem. Soc.* **1977**, *99*, 7926. (b) Ahlberg, P. *Chem. Scr.* **1973**, *3*, 183. (c) Thibblin, A.; Ahlberg, P. *J. Am. Chem. Soc.* **1979**, *101*, 7311. (d) Thibblin, A. *Chem. Scr.* **1980**, *15*, 121. (f) Thibblin, A. *J. Am. Chem. Soc.* **1983**, *105*, 853. (g) Hoffmann, R.; Radom, L.; Pople, J. A.; Schleyer, P. v. R.; Hehre, W. J.; Salem, L. *J. Am. Chem. Soc.* **1972**, *94*, 6221. (h) Apeloig Y.; Rappoport, Z. *J. Am. Chem. Soc.* **1979**, *101*, 5095.

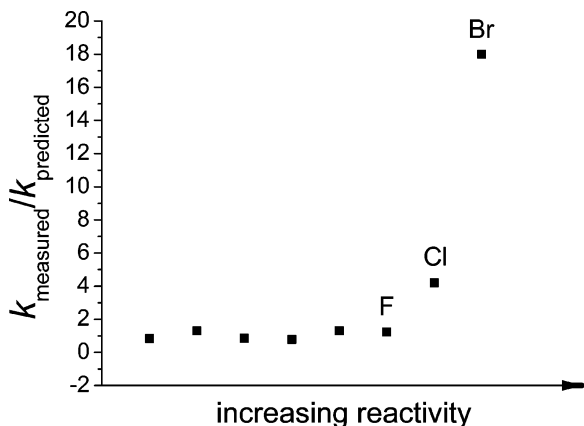


Figure 2. Deviations from the Taft plot: $k_{\text{measured}}/k_{\text{predicted}}$ ratio for H/D exchange for substrates **1–5** and for the elimination reactions of methylated substrates with halogen leaving groups.

fluoroethyl)pyridinium iodide in $\text{OH}^-/\text{H}_2\text{O}$ on the base of the large activation by methylation of the N atom of the pyridine ring (Methyl Activating Factor = 0.87×10^6 , $\text{OH}^-/\text{H}_2\text{O}$, 50 °C, $\mu = 1 \text{ M KCl}$). Tentatively we have also assigned an (E1cb)₁ mechanism¹⁸ with 1-methyl-2-(2-chloroethyl)pyridinium iodide on the base of the large MethylAF = 0.69×10^6 ($\text{OH}^-/\text{H}_2\text{O}$, 25 °C, $\mu = 1 \text{ M KCl}$), but it was recognized²⁰ that an E2 mechanism, with a significant negative charge on the β -carbon, would show a high value of MethylAF. The uncertainty is evident in the mechanistic assignment by these experimental data; therefore, we have approached the problem by a combined experimental and computational study. With substrates activated by the phenylsulfonyl group¹¹ in EtO^-/EtOH , 25 °C, an (E1cb)₁ mechanism was proposed with leaving groups F, Cl, OTs, while an E2 concerted mechanism was assigned with Br, I on the base of the observed deviation in the Taft plot. In systems activated by the 9-fluorenyl group,¹⁵ the deviations from the Taft plot for Cl and Br have been interpreted with an E2 process; with leaving group F a probable E1cb mechanism seems consistent. It is also important to know the $\text{p}K_{\text{a}}$ for the dissociation of the β -H (with respect to the leaving group) of our substrates for elimination reactions, so that it is possible to relate the operating reaction mechanism with these basic properties of the reactant. For 1,2-dimethyl pyridinium a $\text{p}K_{\text{a}}$ of 19.8 has been reported.³⁴ To estimate the effect of a CH_2X group on the K_{a} by Taft correlation, it is necessary to know the value of ρ^*_{eq} . In first the approximation we consider the same value of ρ^*_{eq} used by Jencks^{16b} for the *para*-nitrophenethyl system, $\rho^*_{\text{eq}} = +2.5$. The estimated $\text{p}K_{\text{a}}$ value 1-methyl-2-(2-fluoroethyl)pyridinium iodide $-\log(K_{\text{a}}/10^{-19.8}) = 2.5 \times (1.1 - 0.49)$ is $\text{p}K_{\text{a}} = 18.3$.

Theoretical Study of the Elimination Reactions. To gain detailed insight into the reaction mechanism of the β -elimination reaction in the systems activated by the pyridine ring, we have carried out Density Functional Theory (DFT) calculations on the systems with the F, Cl, and Br leaving groups. Geometry optimizations in solution have been performed on the reagent, carbanion, and product of the β -elimination reaction. To study the effect of methylation at the pyridine nitrogen, we investigated, in the case of the F substituent, the reactions for both

the methylated substrate (Scheme 2 with X = F) and the nonmethylated one. While in our calculations we generally simulated the water solution environment by means of a continuum solvation model, in the case of the methylated fluorine-substituted substrate, we also studied the effect of explicit solvation of the F leaving group on the geometry and stability of the carbanion. Moreover, to investigate the detailed mechanistic features of the β -elimination reaction, its thermodynamics and kinetics, we explicitly considered the basic environment by studying the approach of a OH^- species (solvated by three water molecules) to the methylated F-substituted reagent, leading to the corresponding carbanion and a $4\text{H}_2\text{O}$ cluster. We hereafter label the methylated (nonmethylated) reagent, carbanion, and product as Me-R-X (R-X), Me-C-X (C-X) and Me-P (P), respectively, with X = F, Cl, and Br.

Computational Details and Calibration of the Method. The B3LYP exchange-correlation functional,³⁵ as implemented in the Gaussian03 program package,³⁶ was used throughout the paper, together with a 6-31++G** basis set.³⁷ Unconstrained geometry optimizations were performed in water solution by means of the conductor-like polarizable continuum model (C-PCM)³⁸ using the default UA0 solvation radii. Evaluation of Gibbs free energies in solution was performed following a procedure similar to those employed for the evaluation of absolute $\text{p}K_{\text{a}}$'s.³⁹ Following a thermodynamic cycle, the Gibbs free energy in solution of species *i* (G^i_{sol}) is defined as $G^i_{\text{sol}} = G^i_{\text{vac}} + \Delta G^i_{\text{solv}}$, where G^i_{vac} is the Gibbs free energy of species *i* in vacuo and ΔG^i_{solv} is the free energy of solvation. G^i_{vac} is computed at the geometry optimized in vacuo, followed by frequency calculations to take into account the vibrational contribution to the total partition function. The translational and rotational contributions are evaluated by standard statistical mechanics (particle in a box and rigid rotor models). ΔG^i_{solv} is directly calculated by a C-PCM single-point calculation together with a reference calculation in vacuo, at the geometry optimized in solution.³⁹ We separately checked that using a PCM rather than a C-PCM solvation model on the C-PCM optimized geometries produces negligible differences in ΔG^i_{solv} . Similarly, our results are only marginally affected by the choice of the solvation radii (UA0 vs UAHF).

Transition state structures for the reaction leading to the carbanion intermediate were located by performing full geometry optimizations. The transition state leading to fluoride loss was located by a constrained geometry optimization along an appropriate reaction coordinate.

The accuracy of DFT calculations with sufficiently large basis sets including diffuse functions has previously been found to be comparable to that of correlated ab initio methods when investigating elimination/substitution reactions in $\text{CH}_3\text{CH}_2\text{F}$.^{22d} However, a great sensitivity of DFT results upon the choice of exchange-correlation functional and basis set was also reported.^{22dg}

(34) (a) Cook, M. J.; Katritzky, A. R.; Linda, P.; Tack, R. D. *J. Chem. Soc., Perkin Trans. 2* **1972**, 1295. (b) Cook, M. J.; Katritzky, A. R.; Linda, P.; Tack, R. D. *J. Chem. Soc., Perkin Trans. 2* **1973**, 1080. (c) Cook, M. J.; Katritzky, A. R.; Linda, P.; Tack, R. D. *Chem. Commun.* **1971**, 510.

(35) Becke, A. D. *J. Chem. Phys.* **1993**, *98*, 5648.

(36) Frisch, M. J. et al. *Gaussian 03*, revision B.05; Gaussian, Inc.: Pittsburgh, PA, 2003 (Supporting Information available for complete ref 36).

(37) Ditchfield, R.; Hehre, W. J.; Pople, J. A. *J. Chem. Phys.* **1971**, *54*, 724.

(38) (a) Barone, V.; Cossi, M. *J. Phys. Chem. A* **1998**, *102*, 1995. (b) Cossi, M.; Rega, N.; Scalmani, G.; Barone, V. *J. Comput. Chem.* **2003**, *24*, 669.

(39) (a) Saracino, G. A. A.; Improta, R.; Barone, V. *Chem. Phys. Lett.* **2003**, *373*, 411. (b) Liptak, M. P.; Shields, G. C. *Int. J. Quantum Chem.* **2001**, *85*, 727. (c) da Silva, C. O.; da Silva, E. C.; Nascimento, M. A. C. *J. Chem. Phys.* **1999**, *103*, 11194. (d) da Silva, C. O.; da Silva, E. C.; Nascimento, M. A. C. *J. Phys. Chem. A* **2000**, *104*, 2402.

Table 2. Main Optimized Geometrical Parameters (Å) for the Methylated and Nonmethylated Reagent, Carbanion, and Product

	Me-R-F	R-F	Me-C-F	C-F	Me-P-F	P-F
$C_{\text{py}}-C_1$	1.507 (1.508)	1.514	1.387 (1.398)		1.469	1.476
C_1-C_2	1.529 (1.530)	1.519	1.463 (1.433)		1.341	1.341
C_2-F	1.415 (1.418)	1.426	1.498 (1.612)			

^a Data in parentheses for Me-R-F and Me-C-F refer to the model including two water molecules solvating the F leaving group.

We therefore checked the reliability of our theoretical approach along three lines. First, we investigated the convergence of our results with basis set expansion, carrying out some calculations using the larger aug-cc-pTVZ basis set.⁴⁰ In particular, using the geometries of the Me-R-F and Me-C-F species optimized with the 6-31++G** basis set, we performed a single-point energy evaluation using the aug-cc-pTVZ basis set (713 basis functions for Me-R-F). The energy difference in solution between the bare Me-R-F and Me-C-F species calculated with the 6-31++G** basis set turned out to be only 0.6 kcal/mol higher than the corresponding quantity calculated with the aug-cc-pTVZ basis set, suggesting that our results are reasonably stable with respect to basis set expansion. Second, we performed additional MP2/6-31++G** geometry optimizations in solution on the solvated Me-C-F and Me-C-Cl species to assess the ability of our DFT approach to predict the existence of a stable carbanion intermediate for these two systems; we found both methods to predict the existence of a carbanion in the case of the F leaving group and the absence of a stable intermediate in the Cl case; see below. Finally, we further checked the accuracy of our theoretical approach by calculating the pK_a of the Me-R-F reagent and of 1,2-dimethyl pyridinium, following the standard procedure of ref 39a using the data obtained at the B3LYP/6-31++G** level. For 1,2-dimethyl pyridinium we obtain a pK_a value of 21.1, which matches very well the experimental value of 19.8.³⁴ Similarly, we calculate for Me-R-F a pK_a of 16.1, in good agreement with our estimate of 18.3.

Nuclear Geometries. We start our discussion by analyzing the optimized geometrical structures of the methylated and nonmethylated substrates with the F leaving group. All relative nuclear positions were optimized without constraints in solution, and in Table 2 we report the most relevant resulting geometrical parameters for the various species investigated. The results obtained by considering the explicit solvation of fluorine by two water molecules are also shown in parentheses, and the optimized molecular structures of the methylated species are displayed in Figure 3.

The most remarkable difference between the methylated and nonmethylated substrates is that while for the former we find a stable minimum in correspondence of the carbanionic structure, for the latter no such minimum exists. Indeed, every attempt to locate the optimized geometrical structure of the nonmethylated C-F intermediate resulted in the loss of the fluoride leaving group and the concomitant formation of the olefin product. It may be interesting to note that, by contrast, use of a smaller 6-31g** basis set, which does not include diffuse functions, does lead to a stable C-F intermediate structure. This reflects

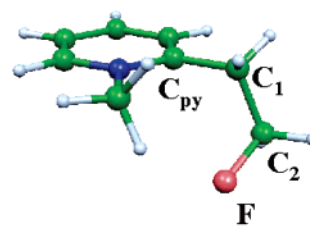
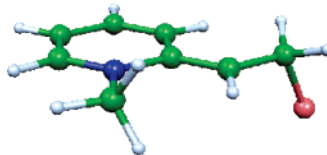
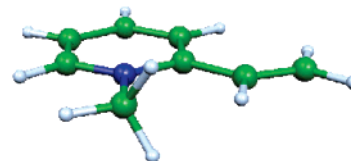
Reagent: Me-R-F**Carbanion: Me-C-F****Product: Me-P**

Figure 3. Optimized molecular structures of the methylated reagent (Me-R-F), carbanion (Me-C-F) and product (Me-P).

the effect of diffuse functions in stabilizing the F^- leaving group. It is also very important that, regardless of the basis set used for the geometry optimizations, a C-F intermediate local minimum is found in vacuo, both for the methylated and nonmethylated systems. Thus, solvation has a crucial effect in the reactions investigated and must be properly accounted for in the theoretical simulations.

For the methylated substrates we notice that while the $C_{\text{py}}-C_1$ and C_1-C_2 distances (see Figure 3) show values close to those of typical single carbon-carbon bonds in the reagent species, in the carbanion a considerable shortening of both parameters takes place, reflecting a high degree of conjugation involving these two carbon-carbon bonds. In particular, the largest variation involves the $C_{\text{py}}-C_1$ bond length (1.507 vs 1.387 Å), which implies a significant effect of the methylated pyridine ligand. On the contrary, the C-F bond length in the carbanion is elongated with respect to the reagent (1.498 vs 1.415 Å, respectively), indicating the weakening of the C_2-F bond which precludes the loss of the halogen leaving group. We notice, moreover, that in the carbanion the plane defined by the C_1-H-C_2 atoms is almost coplanar with the pyridine plane, confirming the expected sp^2 hybridization of the C_1 carbon. We notice that the geometrical parameters of the carbanion are consistent with the enamine structure displayed as the right-hand resonance contributor in Scheme 1. We refer to the intermediate as a carbanion, however, since this term is commonly used to identify the intermediate species in E1cb reactions. For the methylated product of the reaction, an inversion in the relative length of $C_{\text{py}}-C_1$ and C_1-C_2 distances takes place with respect to the carbanion, and the C_1-C_2 distance (1.341 Å) is close to (only slightly larger than) typical double carbon-carbon bond distances.

(40) Woon, D. E.; Dunning, T. H., Jr. *J. Chem. Phys.* **1993**, *98*, 1358.

Aside from the absence of a carbanionic local minimum, our calculations show that the nonmethylated substrates possess structures very similar to those of the corresponding methylated species, with only a slight elongation of the bond lengths considered in Table 2.

Turning now to the methylated species including two water molecules solvating the fluorine, we notice that while the geometry of the reagent is only slightly affected by explicit solvation of the F leaving group (the C₂–F bond is elongated by only 0.003 Å), the carbanion undergoes a considerable elongation of the C₂–F distance, which increases from 1.498 to 1.612 Å. This large variation can be related to the hydrogen bonds formed in the carbanion intermediate between the two water molecules and the F leaving group (HOH...F distances of 1.88 and 1.89 Å), which further weaken the C₂–F bond. In line with these geometrical variations, the calculated Mulliken charges on the fluorine atom in the carbanion increase from –0.42 to –0.46 upon including the two solvating water molecules in our model. It is remarkable, however, that the energy gain associated to this substantial stretching of the C₂–F bond in the carbanion is computed to be only 1.2 kcal/mol. Thus, the looseness of the C₂–F bond (related to the so-called hyperconjugation²⁴) seems to have a significant structural impact but affects only marginally the reactivity of the system. This is in agreement with the experimental alignment of the rate constant for the elimination reaction with 2-(2-fluoroethyl)-1-methylpyridinium iodide in the Taft correlation diagram. The stability of the solvated carbanion intermediate was verified by MP2/6-31++G** geometry optimizations in solution of Me–C–F(2H₂O), which confirmed the existence of a minimum in correspondence of the carbanionic structure, with a slightly shorter C₂–F distance than that calculated by B3LYP (1.536 vs 1.612 Å, respectively).

Reaction Mechanism. To provide a detailed description of the β-elimination reaction mechanism, we investigated the potential energy surface for the reaction between OH[–] and Me–R–F. Since, as discussed above, explicit solvation, in conjunction to the continuum solvation model, is found to influence appreciably the geometry of the Me–C–F intermediate, we adopted the model with two water molecules solvating the F leaving group. Moreover, description of OH[–] basicity also requires proper explicit solvation. Therefore we included three water molecules binding OH[–] in our model. Upon formation of the carbanion intermediate, a proton is transferred from Me–R–F to OH[–], thus leading to the formation of a cluster of four water molecules.

While the thermodynamics of the reaction can be estimated by the difference between the free energies of the isolated Me–R–F(2H₂O) and OH[–](3H₂O) reagents and the Me–C–F(2H₂O) and OH₂(3H₂O) products, the simulation of its kinetics requires us to explicitly consider the interaction of the Me–R–F(2H₂O) and OH[–](3H₂O) reagents along a reaction coordinate (RC). We shall later discuss in detail some essential features of the computed multidimensional potential energy surface, but it is preliminarily quite interesting to analyze the reaction along a chosen RC. Obviously, the choice of a suitable approximate RC is crucial for the proper description of the reaction mechanism, and in the present case, a perfectly natural and adequate procedure is to sample the potential energy surface along the distance of approach of the base to the substrate, since

the base has to attack the reagent in order to abstract a proton. In particular we have chosen the distance between the oxygen of the OH[–] and the C₁–H hydrogen, and at each sampled point, all other geometrical parameters were left free to relax in a geometry optimization. This choice does not introduce any explicit constraint, in particular, on the C₁–H and C₂–F bond distances, whose manner of variation, concerted or stepwise, upon approach of the base, fundamentally characterizes the reaction mechanism. Basically, there are two possibilities: either the base abstracts a proton from Me–R–F leading to the formation of a stable carbanion intermediate (stepwise) or as the base approaches the reagent, the proton abstraction is accompanied by the simultaneous loss of a solvated F group (concerted).

Before proceeding to the analysis of the potential energy surface, we notice that the two hydrogen atoms bound to C₁ have a different electrostatic environment so that a different interaction of the base might be expected when attacking the hydrogen gauche or anti to the fluorine atom. We therefore investigated both attack directions, performing separate constrained geometry optimizations along the gauche and anti C₁–H...OH[–] distances. In both cases, the C₁–H...OH[–] distance was sampled from 2.1 Å, corresponding to a negligible interaction between Me–R–F(2H₂O) and OH[–](3H₂O), to 1.0 Å, roughly corresponding to the value of a H–O bond in a water molecule. We first discuss the anti attack. A series of configurations encountered during the scan of the potential energy along the anti C₁–H...OH[–] distance, with some relevant optimized geometrical parameters, are shown in Figure 4.

As can be noticed from Figure 4, for a long (2.1 Å) value of the RC, the geometry of the Me–R–F(2H₂O) unit is essentially that of the isolated reagent. As OH[–](3H₂O) approaches the C₁–H hydrogen, however, significant changes in the geometry of the Me–R–F(2H₂O) unit take place. In particular, for an RC value of 1.4 Å the C₁–H bond is substantially elongated (1.217 Å), while the C₂–F bond is only slightly longer than in the initial configuration (1.462 Å). For an RC value of 1.35 Å, corresponding to the maximum energy structure in solution along the selected RC, and therefore to the approximate transition state, the C₁–H bond is further elongated (1.289 Å) while the C₂–F bond is still rather short (1.481 Å). Further, reducing the RC leads to breaking of the C₁–H bond and to the formation of the carbanion, loosely solvated by the 4H₂O cluster. Notice that the C₂–F distance in this solvated carbanion structure (1.617 Å) is essentially the same as that in the isolated Me–C–F(2H₂O) optimized structure (1.612 Å), reflecting the negligible perturbation on the structure of the Me–C–F(2H₂O) unit due to the presence of the water cluster. The formation of the solvated carbanion is accompanied, as expected, by an sp³ to sp² change in the C₁ hybridization (see Figure 4). Starting from the maximum energy structure encountered along the RC scan, we have optimized the geometry of the transition state in solution without constraints, finding a structure (TS1) almost identical to the starting one characterized by C₁–H and O...H distances of 1.259 and 1.395 Å.

We then repeated the potential energy surface scan along the gauche C₁–H...OH[–] distance. The geometrical variations along the selected RC are similar to those discussed above for the anti attack. The approximate transition state structure, located also in this case for an RC value of 1.35 Å, resembles that of

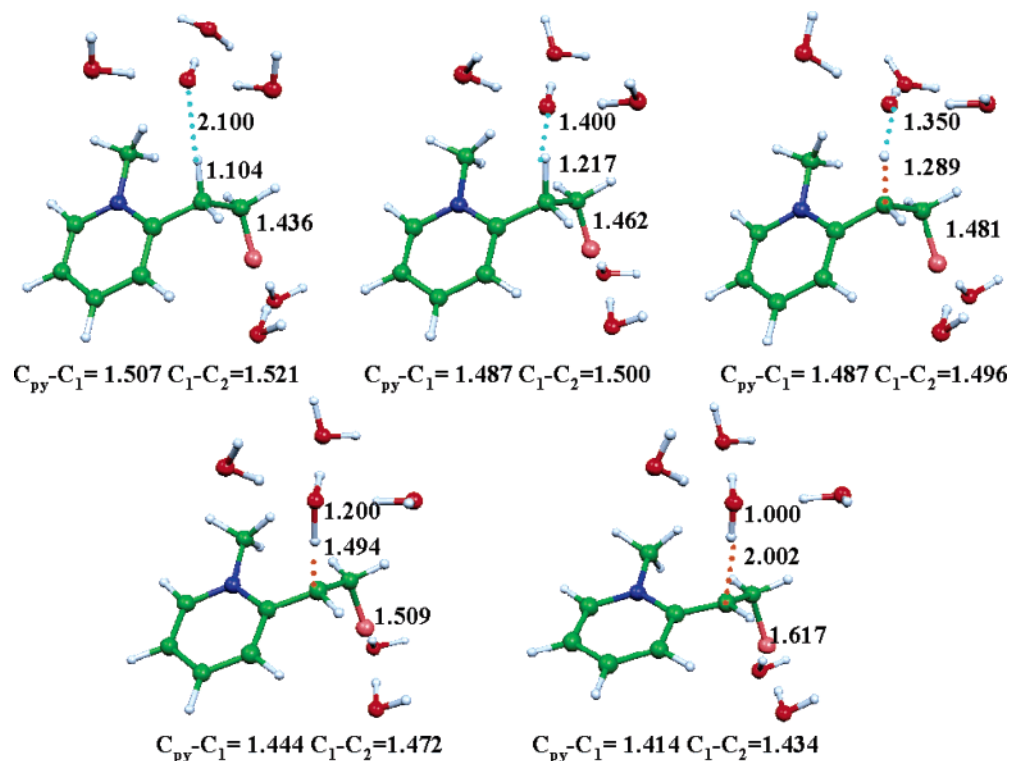


Figure 4. Optimized molecular structures and main geometrical parameters (Å) obtained during the potential energy surface scan along the $C_1-H \cdots OH^-$ approximate reaction coordinate for the methylated substrate with a F leaving group. The bond corresponding to the approximate reaction coordinate is represented in the first three snapshots as a dashed light-blue line. The C_1-H bond, which is being broken, is represented in the last three snapshots as a dashed orange line.

TS1, with C_1-H and C_2-F distances of 1.271 and 1.449 Å, respectively, but is calculated to lie 1.8 kcal/mol above TS1, suggesting that the favored base attack is the one leading to abstraction of the hydrogen anti to the fluorine atom.

We conclude therefore that proton abstraction from $Me-R-F(2H_2O)$ leads to a stable carbanion. We now want to investigate the second step of the reaction, i.e., the elimination of a solvated F group from $Me-C-F(2H_2O)$. Also in this case, an approximate RC has to be defined to scan the potential energy surface of the system and an obvious choice is represented by the C_2-F bond distance. We therefore performed geometry optimizations starting from $Me-C-F(2H_2O)$, constraining the C_2-F bond length to increase from its initial value in $Me-C-F(2H_2O)$ (1.612 Å), up to 2.5 Å, the latter value roughly corresponding to complete dissociation. Following this procedure, an approximate transition state structure (TS2) could be located on the potential energy surface for a value of the approximate RC of 1.75 Å, a value only 0.138 Å larger than the equilibrium value of this parameter in the $Me-C-F(2H_2O)$, suggesting that the intermediate carbanionic structure corresponds to a very shallow minimum, in accord with the observed looseness of the C_2-F bond (see below).

The presence of a minimum in correspondence of the carbanionic intermediate structure and the results of the potential energy surface scan along the two one-dimensional RCs discussed above suggest that the E1cb mechanism represents a viable pathway for the β -elimination reaction in the methylated substrate. To further explore the reaction mechanism for the methylated substrate, we explicitly considered the two-dimensional potential energy surface defined by the independent variations of the C_1-H and C_2-F bond distances and the free optimization of all the other parameters. Models for such

potential energy surfaces illustrating the qualitative relationship between the E2 and E1cb reaction mechanisms were first discussed by More O'Ferrall.⁴¹ We have performed constrained geometry optimizations on a grid of selected values of the two parameters ranging from 1.1 to 2.0 Å for C_1-H and 1.4 to 2.0 Å for C_2-F , relaxing all the other degrees of freedom. The initial and final set of values roughly correspond to formed and broken C_1-H and C_2-F bonds, respectively, and are characteristic of the $Me-R-F$ reagent and of the noninteracting $Me-P$ and $F^-(2H_2O)$ products. This procedure, computationally very expensive due to the large number of constrained geometry optimizations required, should provide a definitive answer regarding the mechanism of the β -elimination reaction. Due to the slightly higher energy barrier calculated for the base approach to the gauche hydrogen, we limited this analysis to the base attack to the hydrogen anti to the fluorine atom.

The results are displayed in Figure 5 and clearly show that a concerted E2-like reaction mechanism can be ruled out for the present system. Indeed, starting from the $Me-R-F$ reagent ($C_1-H = 1.094$, $C_2-F = 1.428$) up to a C_1-H value of 1.3 Å, we notice that stretching the C_2-F bond corresponds to a steep energy increase. Moreover, increasing the C_1-H distance leads to only a slight increase of the C_2-F distance, reflecting the progressive formation of the $Me-C-F$ carbanion intermediate, characterized by a broken C_1-H bond and an elongated C_2-F distance (1.612 Å). The energy increase associated with the C_2-F stretching, however, becomes progressively smaller as the C_1-H distance is further increased. Eventually, for a C_1-H value > 1.8 Å, an almost flat region of the surface is reached, from which the system can either reach the carbanion intermedi-

(41) More O'Ferrall, R. A. *J. Chem. Soc. B* **1970**, 274.

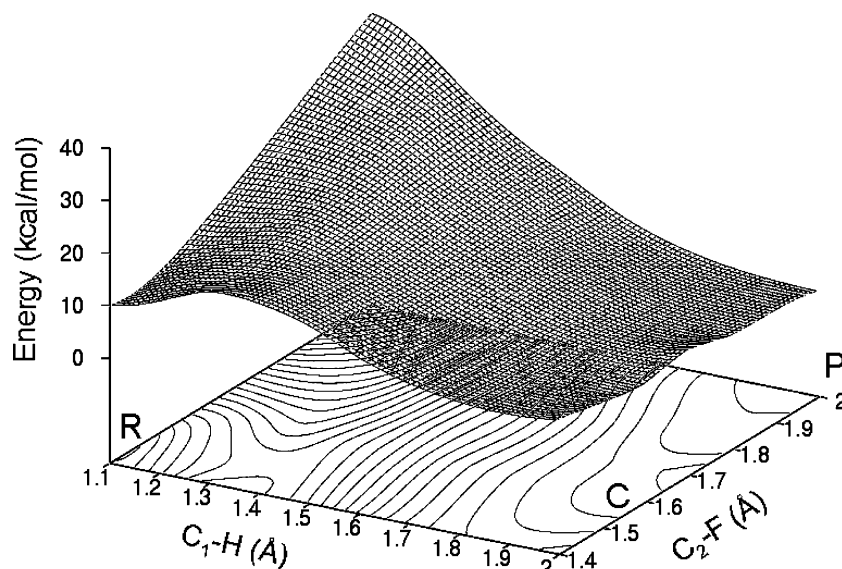


Figure 5. 3D plot and contour plot of the computed potential energy surface for the elimination reaction of the methylated fluorine-containing substrate, as a function of the C_1-H and C_2-F (Å) bond distances.

ate via the energetically favored pathway or surmount the small energy barrier along the C_2-F coordinate leading to the formation of the Me-P product. We may thus conclude that the present Me-R-F system represents a borderline case between the E1cb and E2 reaction mechanisms, with an evident propensity for the former. It is also interesting to notice that the C_1-H and C_2-F distances and the $C_1-H...OH^-$ distance are effectively coupled, so that increasing separately either one of the C_1-H and C_2-F distances leads to a decrease of the $C_1-H...OH^-$ distance. As a consequence, the approximate transition state structure on the bidimensional potential energy surface strictly resembles the approximate TS1 transition state structure located for the monodimensional scan along the $C_1-H...OH^-$ distance, with C_1-H and C_2-F distances of 1.3 and 1.5 Å, respectively, and a $C_1-H...OH^-$ distance of 1.398 Å. This confirms that the $C_1-H...OH^-$ distance is a good approximate RC.

Although the topological features of the reaction potential are qualitatively well illustrated by the energy surface in solution of Figure 5, to obtain a reliable estimate of the reaction energetics, Gibbs free energies in solution must be computed. A schematic display of the Gibbs free energy surface in solution for the β -elimination reaction is reported in Figure 6. For simplicity, activation free energies were calculated from the approximate transition state structures obtained from the monodimensional scans along the C_1-H and C_2-F distances. Thermodynamic parameters are calculated from the sum of the free energies of the isolated systems.

As Figure 6 shows, we calculate a Gibbs free energy barrier of 21.1 kcal/mol in correspondence of the formation of the solvated carbanion intermediate from the isolated solvated reagents. This free energy barrier is dominated by the high entropic contribution which accompanies the bimolecular formation of the transition state from the isolated reagents.

Once the initial barrier is overcome, the system can evolve via the formation of the carbanion intermediate (and four water molecules), which is calculated to lie 9.5 kcal/mol above the starting reagents. From the carbanionic intermediate the system can then easily evolve toward the formation of the olefin product

by loss of a solvated F^- group, overcoming a small Gibbs free energy barrier of only 2.8 kcal/mol. The final products of the reaction are located 21.8 kcal/mol below the Gibbs free energy of the solvated carbanion; we therefore expect the formation of the final products from the carbanion intermediate to be a favored (and fast) reaction, due to the low energy barrier and the quite high exothermicity.

We notice that the thermodynamics of the reaction leading to formation of the carbanion could be obtained by combining the experimental pK_a estimate of Me-R-F (18.3) and that of OH^- ($pK_w=14.0$), according to $\Delta G = 2.303RT (pK_a - pK_w)$. Doing so results in a Gibbs free energy difference between Me-R-F + OH^- and Me-C-F + H_2O of 5.9 kcal/mol. Even though this value is not directly comparable to the computed result because our model explicitly includes water molecules, it seems clear that the theoretical value of 9.5 kcal/mol overestimates the experimental ΔG . Since our computational model allows us to almost exactly reproduce the estimated pK_a of Me-R-F (see computational details), we conclude that the main source of inaccuracy in our calculations resides in the underestimation of OH^- basicity. This error is also likely to have an impact on the computed free energy barrier of 21.1 kcal/mol, which is higher than the experimental estimate (16.1 kcal/mol). That the computed result may overestimate somewhat the activation barrier, on the other hand, is not unexpected also on other grounds, since we estimate thermal corrections to the Gibbs free energy in vacuo, and the entropic contribution is essentially dominated by the loss of the translational and rotational degrees of freedom related to the associative character of the transition state. In addition, a general overestimation of the activation energies results from having located approximate transition state structures as maxima along chosen reaction coordinates. In conclusion the analysis of the Gibbs free energy landscape clearly indicates that the reaction with the F leaving group occurs via an E1cb irreversible mechanism. Indeed, the computed barrier for the backward reaction from the carbanion (11.6 kcal/mol) is much higher than that for fluoride loss from the carbanion (2.8 kcal/mol).

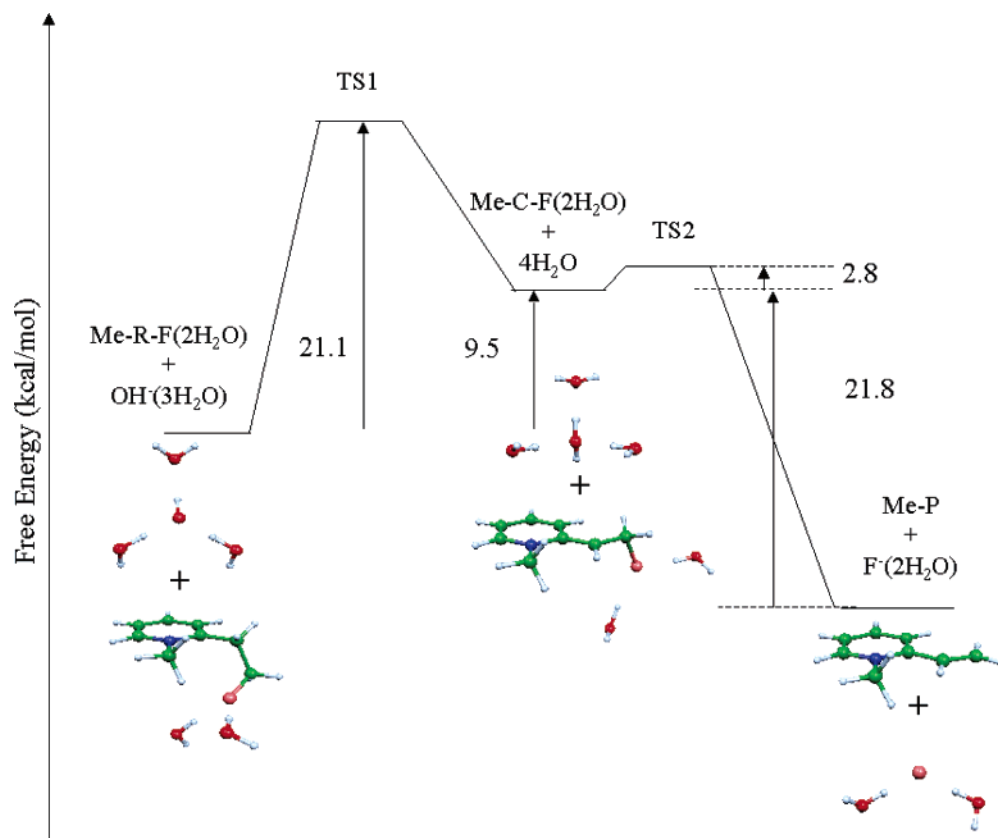


Figure 6. Schematic representation of the calculated Gibbs free energy surface in solution (kcal/mol) for the β -elimination reaction between solvated Me-R-F and OH⁻.

We finally extended our calculations to the methylated systems having Cl and Br as leaving groups. For the Cl methylated substrate we used the same 6-31++G** basis set used above, while for the Br methylated substrate we used an aug-cc-pVDZ basis set, due to the absence of the 6-31++G** basis set for the Br atom. Geometry optimizations were performed on the reagent and carbanion. Remarkably, while for the F methylated substrates we have found a local minimum energy structure for the carbanion intermediate, for both the Cl and Br methylated substrates, every attempt to optimize the geometry of the carbanion intermediate resulted in the loss of the chloride and bromide leaving groups, leading directly to the olefin product. The absence of a minimum for the carbanion intermediate with a Cl leaving group was confirmed by MP2/6-31++G** geometry optimizations performed on this system. The absence of a carbanion intermediate for the Cl and Br methylated substrates indicates that the β -elimination reactions in these systems proceed via a concerted E2 reaction mechanism. To gain further insight into the reaction pathway in the Cl methylated case, we performed constrained geometry optimizations for the Me-C-Cl(2H₂O)/OH₂(3H₂O) system, along the same reaction coordinate described above for the F case (C₁-H...OH⁻ distance). A series of configurations encountered during the scan of the potential energy along the anti C₁-H...OH⁻ distance, with some relevant optimized geometrical parameters, are available as Supporting Information. The results show that the reaction pathway is initially similar to that calculated for the F case. Reducing the C₁-H...OH⁻ distance from 2.1 to 1.3 Å (the latter value corresponding to the approximate transition state) leads to an increase of the C₂-Cl distance from 1.84 to 1.92 Å. Further reduction of the ap-

proximate RC, however, leads to a rapid increase of the C₂-Cl distance: for RC = 1.2 Å the C₂-Cl distance is 2.22 Å, and for RC = 1.1 Å the carbon-chlorine is essentially broken (C₂-Cl = 2.73 Å). These results suggest that there is continuity between the E1cb and E2 reaction mechanisms in the F and Cl cases. The lack of a net distinction between the E1cb and E2 reaction mechanisms in these borderline cases is confirmed by the calculated approximate energy barrier (total energy in solution) along the selected RC which in the Cl case is only 0.7 kcal/mol lower than the corresponding value calculated for the F substrate. This result is satisfactorily consistent with the observed similarity in the reaction rates for the F and Cl methylated substrates. It is also in essential agreement with the proposal of Jencks,^{13b} according to which the barrier for leaving group expulsion from the carbanion tends to disappear with increasingly better leaving groups (Br > Cl > F) and the intermediate has no significant lifetime.

Conclusions

In the present work we have combined the information obtained by experimental measurements with detailed theoretical calculations, to definitively characterize the mechanism of base-induced β -elimination reactions in systems activated by the pyridyl ring. In particular, our attention has focused on some borderline cases with halogen leaving groups, where it was uncertain if the reaction proceeds via a carbanion intermediate which subsequently expels the halide (E1cb mechanism) or the simultaneous concerted loss of a proton and the halide group takes place (E2 mechanism) upon base attack.

Application of the Taft equation for isotope exchange with noneliminating nitrogen-methylated substrates (1–5) allowed

us to predict the rate of carbanion formation in the elimination reactions when the leaving group is F, Cl, or Br. Comparison of the rate constants for the related β -elimination reactions induced by OH^- suggests that with the F leaving group the mechanism is E1cb irreversible, while with Cl and Br deviations from the Taft equation are observed.

The theoretical simulations prove that the elimination reaction proceeds via formation of a moderately stable carbanion in the case of a fluoride leaving group for the *N*-methylated substrate. This carbanion, however, has a very small barrier (2.8 kcal/mol) to fluoride loss and is therefore expected to be a very short-lived transient intermediate. By contrast, a concerted mechanism with no stable carbanion intermediate takes place in the case of the chloride and bromide leaving groups. Similarly, for the nonmethylated substrate with a F leaving group, our calculations indicate that there is no stable minimum in correspondence of a carbanion intermediate, thus suggesting for this substrate an E2 reaction mechanism. We remark that calculations in vacuo predict a stable carbanion intermediate regardless of the basis set quality, the same result obtained by calculations in solution with a basis set which does not include diffuse functions. These results show the importance of solvation and of basis sets including diffuse functions for an accurate description of β -elimination reactions in the present systems.

The picture emerging from the theoretical analysis is in agreement with the experimental data, which show, for the *N*-methylated substrate with a F leaving group, a reactivity pattern in line with the occurrence of an E1cb reaction mechanism. The increased stability of the carbanion intermediate upon methylation of the pyridine nitrogen for the substrate with

a F leaving group is related to the high degree of conjugation involving the *N*-methylated pyridine ring and the $\text{C}_{\text{py}}-\text{C}_1$ and C_1-C_2 carbon-carbon bonds.

Interestingly, the methylated substrate with Cl leaving group shows only a moderate increase in reactivity compared to the substrate with F leaving group, despite the lack of a stable carbanion calculated for this system. That this change in reaction mechanism is not necessarily accompanied by a significant increase in the reaction rate is not surprising, if one considers the details of the potential energy surface calculated for the F substrate and the similarity of the energy barrier calculated for the Cl substrate. These results show the lack of a net distinction between the E1cb and E2 reaction mechanisms in these borderline cases: the energy barrier for halide expulsion is initially very high but drops progressively to nearly zero as the proton leaves the substrate to be transferred to the base. At this point, the carbon-halide bond becomes very loose, and the energy surface flat, so that the halide group may begin leaving the substrate with a small or negligible energy barrier.

Acknowledgment. Thanks are due to the Italian Ministero dell'Istruzione, dell'Università e della Ricerca (MIUR) for financial support.

Supporting Information Available: Experimental details, full refs 13d and 36. Figure showing the reaction pathway for the Cl-methylated system. Optimized molecular structures and energies of relevant stationary points. This material is available free of charge via the Internet at <http://pubs.acs.org>.

JA0539138